AD-A121 106 RESIDUAL STRENGTH CHARACTERIZATION OF LAMINATED COMPOSITES SUBJECTED TO IMPACT LOADING(U) AIR FORCE MATERIALS LAB WRIGHT-PATTERSON AFB OH

1/1

UNCLASSIFIED G E HUSMAN ET AL. FEB 74 AFML-TR-73-309 F/G 11/4 NL

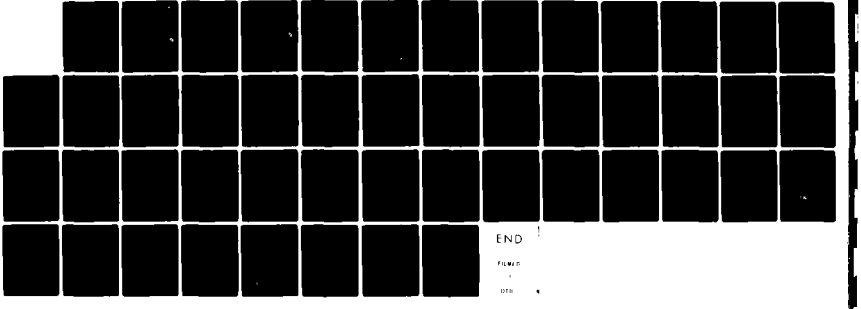

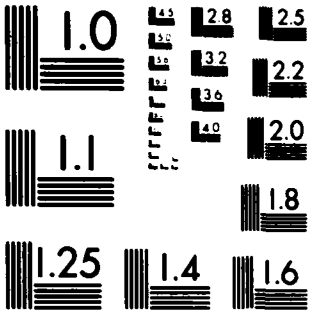

MICROCOPY RESOLUTION TEST CHART
NATIONAL BUREAU OF STANDARDS-1963-A

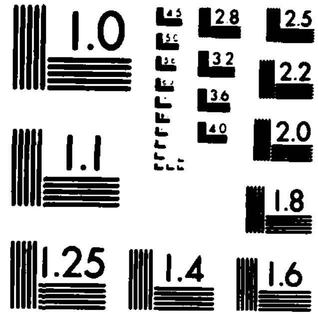

MICROCOPY RESOLUTION TEST CHART
NATIONAL BUREAU OF STANDARDS-1963-A

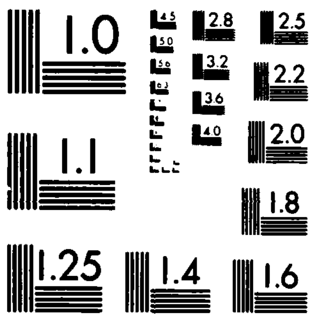

MICROCOPY RESOLUTION TEST CHART
NATIONAL BUREAU OF STANDARDS-1963-A

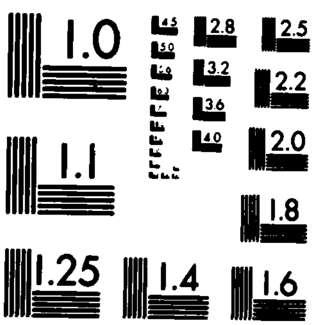

MICROCOPY RESOLUTION TEST CHART
NATIONAL BUREAU OF STANDARDS-1963-A

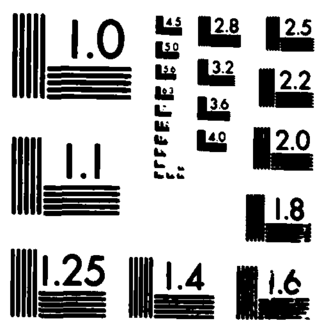

MICROCOPY RESOLUTION TEST CHART
NATIONAL BUREAU OF STANDARDS-1963-A

AFML-TR-73-309

RESIDUAL STRENGTH CHARACTERIZATION OF LAMINATED COMPOSITES SUBJECTED TO IMPACT LOADING

G. E. HUSMAN
J. M. WHITNEY
J. C. HALPIN

TECHNICAL REPORT AFML-TR-73-309

FEBRUARY 1974

AIR FORCE MATERIALS LABORATORY
AIR FORCE SYSTEMS COMMAND
WRIGHT-PATTERSON AIR FORCE BASE, OHIO 45433

NOTICE

When Government drawings, specifications, or other data are used for any purpose other than in connection with a definitely related Government procurement operation, the United States Government thereby incurs no responsibility nor any obligation whatsoever; and the fact that the government may have formulated, furnished, or in any way supplied the said drawings, specifications, or other data, is not to be regarded by implication or otherwise as in any manner licensing the holder or any other person or corporation, or conveying any rights or permission to manufacture, use, or sell any patented invention that may in any way be related thereto.

Copies of this report should not be returned unless return is required by security considerations, contractual obligations, or notice on a specific document.

AIR FORCE/56780/18 April 1974/200

AFML-TR-73-309

RESIDUAL STRENGTH CHARACTERIZATION OF LAMINATED COMPOSITES SUBJECTED TO IMPACT LOADING

G. E. HUSMAN
J. M. WHITNEY
J. C. HALPIN

FOREWORD

This report was prepared by G. E. Husman of the Composites and Fibrous Materials Branch, and J. M. Whitney and J. C. Halpin of the Mechanics and Surface Interactions Branch, Nonmetallic Materials Division, Air Force Materials Laboratory. The work was conducted under Project No. 7340, "Nonmetallic and Composite Materials", Task No. 734003, "Structural Plastics and Composites", and was administered by the Air Force Materials Laboratory, Air Force Systems Command, Wright-Patterson Air Force Base, Ohio.

This report covers work conducted during the period of July 1972 through November 1973. This report was released by the authors in December 1973.

The authors wish to acknowledge Mr. T. W. Lee of the University of Dayton Research Institute for performing the ballistic impact tests.

This report has been reviewed and is approved.

T. J. REINHART, JR., Chief
Composites and Fibrous Materials Branch
Nonmetallic Materials Division
Air Force Materials Laboratory

ABSTRACT

An analogy between damage inflicted by a single point hard particle impact and damage inflicted by inserting a flaw of known dimensions in a static tensile coupon is discussed. The results suggest that residual strength can be predicted as a function of kinetic energy of impact by executing two experiments, a static tensile test on an unflawed specimen and a static tensile test on a coupon previously subjected to a single point impact. The model appears to be accurate for impact velocities which are less than the penetration velocity. For velocities above complete penetration, the residual strength is identical to the static strength of a coupon with a hole having the same diameter as the impacting particle. Comparison of various materials indicates that the impact strength of composite materials is strongly influenced by the strain energy to failure of the reinforcement.

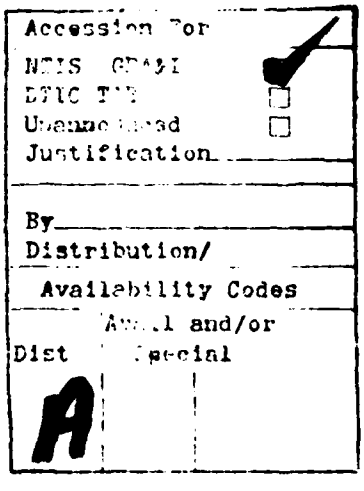

TABLE OF CONTENTS

ILLUSTRATIONS

SECTION I

INTRODUCTION

Static residual strength is usually defined as the failure stress in a uniaxial tension test performed after the specimen has been subjected to some previous load history. Such information is a useful measure of damage and can be used in predicting the life expectancy of a composite material subjected to a specified load history [1]. In a similar manner, residual strength should be a useful measure of damage in a composite subjected to a local impact load, as well as a means of screening materials for potential application in structures subjected to an impact load such as turbine engine fan blades.

It has been previously noted [2] that a hole in a composite material inflicted by a bullet produces the same reduction in static strength as a drilled hole of the same diameter as the bullet. This is illustrated in Figure 1 for boron-epoxy, graphite-epoxy, and glass-epoxy laminates. Thus, an example exists in which the damage inflicted by a local hard particle impact can be equated, in terms of residual strength, to damage inflicted by an artificially implanted stress concentration.

Now consider a tensile coupon subjected to a localized hard particle impact at a velocity which is less than the penetration velocity. If this specimen is then loaded to failure, the resulting strength will be less than the original tensile strength. This is exactly the same result

produced by implanting a small through-the-thickness crack in a tensile coupon and then stressing it to failure. Thus, if a procedure can be developed for converting the impact damage, in terms of residual strength, to an equivalent crack of known dimensions, the residual strength can be analyzed in terms of a current fracture mechanics model. Such an analogy is developed and executed in the present paper. Comparison between the model and experimental data shows good agreement. The model is also used to compare the local impact resistance of various types of composite materials.

SECTION II

ANALYSIS

Consider a plate of orthotropic construction containing a narrow slit of length 2c perpendicular to a uniform tensile stress, $\bar{\sigma}$, applied at infinity. The critical strain energy release rate, G_{1c}, has been determined by Sih, Paris, and Irwin [3][3]

$$G_{1c} = K_{1c}^2 \left\{ \left(\frac{\bar{S}_{11}\bar{S}_{22}}{2} \right) \left[\left(\frac{\bar{S}_{22}}{\bar{S}_{11}} \right)^{1/2} + \frac{2\bar{S}_{12} + \bar{S}_{66}}{2\bar{S}_{11}} \right] \right\}^{1/2} \tag{1}$$

where K_{1c} is the critical stress intensity factor and $\bar{S}_{ij}$ are orthotropic plate compliances. For a slit in an orthotropic plate, the value of K_{1c} is the same as for an isotropic material [3], i.e.,

$$K_{1c} = \bar{\sigma}\sqrt{\pi c} \tag{2}$$

Substituting Eq. (2) into Eq. (1) yields the result

$$G_{1c} = A c \bar{\sigma}^2 \frac{\bar{S}_{22}}{2} \tag{3}$$

where

$$A = \pi \left\{ \frac{2\bar{S}_{11}}{\bar{S}_{22}} \left[\left(\frac{\bar{S}_{22}}{\bar{S}_{11}} \right)^{1/2} + \frac{2\bar{S}_{12} + \bar{S}_{66}}{2\bar{S}_{11}} \right] \right\}^{1/2} \tag{4}$$

For an isotropic material Eq. (4) reduces to

$$A = 2\pi \tag{5}$$

---

[3] In Reference 3, the x_1 axis is parallel to the crack.

A cursory examination of Eq. (3) reveals that the last two terms on the right-hand side constitute the work/unit volume, W_b, necessary to break the specimen, i.e., the area under the stress-strain curve as determined from the strain field at a distance from the slit. Thus,

$$G_{1c} = A c W_b \tag{6}$$

For an isotropic material, Eq. (5) in conjunction with Eq. (6) yields

$$G_{1c} = 2\pi c W_b \tag{7}$$

It is interesting to note that Rivlin and Thomas [4] have shown that Eq. (7) is applicable to the small deformations of isotropic materials with nonlinear constitutive relations, the nonlinearity being accounted for by the strain energy density term. Thus, it is strongly suspected that Eq. (6) is applicable to orthotropic materials with nonlinear constitutive relations. This means that Eq. (6) represents a very useful form of the strain energy release rate.

Now let us assume that a damage zone adjacent to a stress concentration constitutes a characteristic volume of material which must be stressed to a critical level before fracture. Physically such a zone represents an area of crazing and delamination in a composite material, as discussed previously by Halpin, Jerina, and Johnson [1]. Furthermore, it is assumed that this volume of material is identified by a characteristic dimension, or effective flaw, c_o. In the absence of a mechanically

implanted flaw, it is assumed that this effective flaw determines the strength of laminated composites. Under these assumptions Eq. (6) can also be written in the form

$$G_{Ic} = A c_o W_s \tag{8}$$

where W_s is the energy under the stress-strain curve for statically loaded composites without a mechanically implanted flaw.

Using the damage zone, c_o, in the same manner as the plastic zone approximation of Irwin [5], an effective half crack length $c + c_o$ is assumed for analyzing a slit in a composite material. With this assumption Eq. (6) becomes

$$G_{Ic} = A(c + c_o) W_b \tag{9}$$

Equation (8) now becomes a special case of Eq. (9), i.e., the unflawed strength is recovered as $c \to 0$. This model yields the following relationship for residual strength σ_R in terms of initial unflawed strength σ_o [6]

$$\sigma_R = \sigma_o \sqrt{\frac{c_o}{c + c_o}} \tag{10}$$

It is now desired to derive an analogy, in terms of residual strength, between the local damage inflicted by a small hard particle impact and damage inflicted by implanting a crack of known dimensions in a static tensile coupon. When a plate is subjected to a local hard particle impact, the damage inflicted will be a complex function of the actual impact event. From a practical standpoint, however, it is suspected that for impact velocities less than the penetration velocity, the degree of damage is strongly influenced by the amount of kinetic energy imparted to the plate. Such an assumption is the basis of the Izod or Charpy impact test, and is used in developing the desired analogy. In particular, it is assumed that the difference between the energy density required to break an undamaged specimen and the energy density required to break an impacted specimen is directly proportional to the kinetic energy imparted to the specimen, W_{KE}, dissipated over some volume of the specimen. Thus,

$$W_s - W_b = k \frac{W_{KE}}{V} \tag{11}$$

where V is an unknown volume over which the kinetic energy is dissipated. A complex analysis of the exact impact event would be necessary to determine V theoretically. It is further assumed, however, that this volume can be characterized by some characteristic surface area, A_e, which is independent of the kinetic energy of impact, and the plate thickness, t. Equation (11) can now be written in the form

$$W_s - W_b = K\overline{W}_{KE} \tag{12}$$

or in a more useful form

$$W_b = W_s - K\overline{W}_{KE} \tag{13}$$

where

$$K = \frac{k}{A_e}, \qquad \overline{W}_{KE} = \frac{W_{KE}}{t}$$

To find a relationship between the impact damage and a mechanically induced crack, Eq. (12) is substituted into Eq. (9) with the result

$$G_{1c} = A(c + c_o)(W_s - K\overline{W}_{KE}) \tag{14}$$

Eq. (14) is now equated to Eq. (8) and the results solved for c, yielding

$$c = \frac{c_o K\overline{W}_{KE}}{(W_s - K\overline{W}_{KE})} \tag{15}$$

Substituting Eq. (15) into Eq. (10) yields the desired relationship for residual strength in terms of the impact kinetic energy, i.e.,

$$\sigma_R = \sigma_o \sqrt{\frac{W_s - K\overline{W}_{KE}}{W_s}} \tag{16}$$

Equation (16) suggests that residual strength can be predicted as a function of kinetic energy of impact by executing two experiments, a static tensile test on an unflawed specimen and a static tensile test on a coupon

previously subjected to a single point impact. If the specimen is sufficiently wide so that the impact damage is reasonably well localized the K factor should be independent of specimen geometry. The value of K may, however, depend on laminate stacking sequence and boundary conditions of the experiment (e.g., cantilever specimen versus both ends clamped). It should be noted that if one assumes the impact damage zone to be analogous in residual strength to a specimen with a circular hole instead of a crack, the Bowie fracture model used by Waddoups, Eisenmann, and Kaminski [6] will yield Eq. (16). Thus, the form of Eq. (16) may not depend on the assumed geometry used to develop the analogy. It is important to note that the present analogy depends on the validity of the model used to derive Eq. (10). Data exists in the literature [1, 6] which indicates that such a model has validity for interpreting composite laminate residual strength in the presence of a crack.

Since one of the key parameters in Eq. (16) is W_s, theoretical methods which predict the area under the static stress-strain curve are useful in local impact damage studies. Such a method for approximating W_s has been developed by Petit and Waddoups [7]. This technique, including example calculations, is discussed in the Appendix.

For impact velocities equal to or greater than the velocity for complete penetration (i.e., the impact produces a clean hole) the residual strength becomes independent of the impact event. Thus, for local impact damage the residual strength never vanishes, but reaches a lower limit when the

impact produces a hole. Based on the data in Figure 1, this cut-off value of σ_R can be estimated by drilling a hole of the same diameter as the impacting particle in the laminate being characterized and measuring the residual strength. In actual practice the residual strength will drop below this cut-off as initial penetration, i.e., penetration without producing a complete hole, will cause more damage by removing material around the hole than will be caused when the velocity is high enough to produce a clean hole. Thus, there is a range of impact kinetic energies for which the residual strength undergoes a transition from the damage model represented by Equation (16) and complete penetration as represented by a through hole. This concept is illustrated in Figure 2.

For a better physical understanding of the analogy represented by Eq. (16), the basic concepts are pictorially illustrated in Figure 3.

SECTION III

EXPERIMENTAL PROCEDURE

Composite laminates were impacted with 0.177 inch and 0.25 inch diameter spherical steel projectiles at several velocities and then the residual tensile strength of the damaged specimens measured. The specimens used in the initial portion of this study were 6 inch x 0.5 inch straight sided tensile coupons with fiberglass tabs bonded to the ends for gripping. Most specimens were 12 plies thick (0.1 inch - 0.144 inch depending on the material), and all were [0°, 90°] symmetric laminates. This orientation was chosen for simplicity, and is representative of engineering laminates. The specimens were mounted as cantilever beams and impacted normal to the surface at the center.

A tube with a bore diameter considerably larger than the sphere diameter was used to launch the projectiles, and a plastic sabot or cup protected them from the tube walls and provided a smooth, flat rear face for efficient launch acceleration.

The launcher used either compressed air or burning powder to provide the accelerating pressure. In general, the compressed air assembly was used to launch up to velocities of about 600 ft/sec and powder was used above that. The launcher is capable of a maximum velocity of about 9,000 ft/sec.

At velocities below about 500 ft/sec the compressed gases were vented through slots in the sides of the launch tube and the sabot was caught at the

end of the tube allowing the projectile to travel on alone without hindering the experiment. For velocities above 500 ft/sec the sabot often shattered when abruptly decelerated, causing sabot fragments to follow the projectile to the target thus interfering with the experiment. This difficulty was overcome by slightly drag decelerating the sabot to separate it from the unimpeded projectile and then deflecting it away from the flight path.

The method chosen to measure the velocity of the projectile was very simple but effective. The beams of two inexpensive, low power He-Ne lasers were directed across the flight path. When the projectile interrupted the first beam the high speed counter started. When the second beam was interrupted, the counter stopped. The counter operating at a known frequency gave the travel time over a carefully measured distance between the laser beams. A schematic of the test set-up is illustrated in Figure 4. High speed film was used to determine rebound velocity. Since the projectile underwent very little deformation due to impact, the kinetic energy transmitted to the specimen could be determined from the rebound velocity.

After the specimens were impacted, the damage was visually inspected and then the specimens were tested to failure in tension. A standard 10,000 lb capacity Instron was used for tensile testing with a cross-head speed of 0.05 inches/minute.

SECTION IV

DISCUSSION

The test procedure outlined was used to evaluate several composite material systems to determine the effects of constituent properties on the impact response of a composite. The fibers and resins evaluated and their tensile properties are listed in Table 1. Equation (16) was used to assess the accuracy of the impact analogy. In particular, K was determined by fitting the data to the theory at one value of the kinetic energy. A measured value of W_s was then used in conjunction with Equation (16) to predict values of σ_R/σ_O as a function of $\overline{W}_{KE}$. Thus, an estimate of the residual strength curve is obtained without determining k or A_e.

The experimental results indicated little or no change in impact response due to variations of matrix properties for the resin systems evaluated. This is illustrated in Figure 5 for Modmor II fiber with three different matrix materials having various strains to failure. The solid line represents theoretical results obtained from Equation (16) in conjunction with the procedure previously described. Similar results were obtained with A-S fiber in both epoxy and thermoplastic matrix materials (Table 2). Although the residual strength curves were unchanged, it should be noted that the thermoplastic matrix composites displayed significant differences in failure mode. The thermoplastic matrix composites displayed a denting mode of damage with no delamination, while all of the epoxy laminates displayed local crushing, cracking, and delamination.

Significant changes in impact response due to variations of fiber properties was apparent. This is clearly illustrated in Figure 6 which shows the impact response, using Equation (16) as previously discussed, of the different graphite fibers evaluated and also E-glass. All of these materials had the same epoxy matrix except for the glass which was Scotchply/1002 material. This data agrees well with the results of Novak and DeCrescente [8], and Chamis, Hanson, and Serafini [9]. The impact response of composites appears to be primarily controlled by the strain energy at failure of the fibers, i.e. the combination of high strength and high strain properties in a fiber provide composites with higher resistance to impact damage.

In general, all of the experimental data agreed reasonably well with the response predicted by the model as illustrated in Figures 7 and 8. There was, however, some concern that 1/2 inch wide specimens were too narrow and that the data was being affected by edge conditions, i.e., the specimen was not wide enough for the damage area to be classified as a flaw in an infinite plate. Therefore, a series of A-S/4617 specimens one inch wide were evaluated. In addition, two laminate thicknesses were evaluated to determine if K was independent of thickness. A cursory examination of the results in Figure 7 shows that the K factor is not significantly affected by thickness, but is affected by the smaller width.

In order to more completely define a proper ratio of specimen width to projectile diameter, a series of impact experiments were performed on Scotchply/1002 material using two projectile diameters and specimen widths up to 1-1/2 inches. Results in Figure 8 show that a single value of K can

adequately describe the data for $W/d > 5$. It is important to note in both Figures 7 and 8 that the damage process is slowed considerably by assuring that a local impact occurs. The actual variation of K with W/d is illustrated in Figure 9.

SECTION V

CONCLUSIONS

An analogy in terms of residual strength has been developed between damage inflicted by a localized single point hard particle impact and damage inflicted by inserting a flaw of known dimensions in a static tensile coupon. The procedure allows the local impact resistance of laminated composites to be characterized on at least a comparative basis with a minimum of experimental data. The analogy is applicable to velocities which are less than the velocity of significant penetration. For penetration the residual strength can be characterized as a laminate containing a hole of the same diameter as the impacting particle. Comparison of experimental data to the theory shows good agreement.

Several aspects of the procedure, however, need to be pursued further. In particular, more data is necessary to determine the effect of impact boundary conditions on K. In addition, the procedure needs to be applied to laminate orientations other than $[0°, 90°]_s$ and to various stacking sequences of the same ply orientations.

APPENDIX

STIFFNESS AND FRACTURE PREDICTIONS USING LAMINATION THEORY AND MAXIMUM STRAIN FAILURE CRITERION

Lamination theory can be used to predict the stiffness of a laminate. As the laminate is loaded to failure individual ply failures occur until the last ply fails. As a ply fails the stiffness of the laminate decreases and must be recalculated by deleting the ply which has failed from the calculation. Thus, by using lamination theory to predict laminate stiffness and a failure criterion to predict ply failure, a stress strain curve for the laminate can be approximated and the ultimate strength and work to break predicted. The results of this calculation may then be used to estimate the effective strain energy rate and fracture toughness for a Mode I failure process.

The engineering properties characteristic of an orthotropic ply are used to determine the plane stress moduli of laminated plate theory.

Engineering Properties:

$E_{11} = 21 \times 10^6$ psi

$E_{22} = 1.7 \times 10^6$ psi

$G_{12} = 0.6 \times 10^6$ psi

$\nu_{12} = 0.28$

$\nu_{21} = \nu_{12} E_{22}/E_{11} = 0.0226$

Plane Stress Moduli:

$$Q_{11} = E_{11}/(1 - \nu_{12}\nu_{21})$$

$$= 21.2 \times 10^6 \text{ psi}$$

$$Q_{22} = E_{22}/(1 - \nu_{12}\nu_{21})$$

$$= 1.71 \times 10^6 \text{ psi}$$

$$Q_{12} = \nu_{21} Q_{11} = 0.48 \times 10^6 \text{ psi}$$

$$Q_{16} = 0$$

$$Q_{26} = 0$$

$$Q_{66} = G_{12} = 0.65 \times 10^6 \text{ psi}$$

The plane stress moduli for each ply must be transformed to the orientation of the ply in the laminate.

Transformed Plane Stress Moduli:

$$\overline{Q}_{11} = Q_{11} \cos^4\theta + 2(Q_{12} + 2Q_{66}) \sin^2\theta \cos^2\theta + Q_{22} \sin^4\theta$$

$$\overline{Q}_{22} = Q_{11} \sin^4\theta + 2(Q_{12} + 2Q_{66}) \sin^2\theta \cos^2\theta + Q_{22} \cos^4\theta$$

$$\overline{Q}_{12} = (Q_{11} + Q_{22} - 4Q_{66}) \sin^2\theta \cos^2\theta + Q_{12}(\sin^4\theta + \cos^4\theta)$$

$$\overline{Q}_{66} = (Q_{11} + Q_{22} - 2Q_{66}) \sin^2\theta \cos^2\theta + Q_{66}(\sin^4\theta + \cos^4\theta)$$

$$\overline{Q}_{16} = (Q_{11} - Q_{12} - 2Q_{66}) \sin\theta \cos^3\theta + (Q_{12} - Q_{22} + 2Q_{66}) \sin^3\theta \cos\theta$$

$$\overline{Q}_{26} = (Q_{11} - Q_{12} - 2Q_{66}) \sin^3\theta \cos\theta + (Q_{12} - Q_{22} + 2Q_{66}) \sin\theta \cos^3\theta$$

For the plies of a $(0, 90)_s$ laminate:

θ	0^o	90^o
$\overline{Q}_{11}$	21.2×10^6	1.71×10^6
$\overline{Q}_{22}$	1.71×10^6	21.2×10^6
$\overline{Q}_{12}$	0.48×10^6	0.48×10^6
$\overline{Q}_{16}$	0	0
$\overline{Q}_{26}$	0	0
$\overline{Q}_{66}$	0.65×10^6	0.65×10^6

The stiffness of the laminate is obtained by summing the plane stress moduli through the thickness in proportion to the percentage of the thickness the k^{th} ply occupies of the n ply laminate.

$$\overline{A}_{ij} = \sum_{k=1}^{n} \overline{Q}_{ij}^{k} a^k$$

where

a^k = $\Delta h^k / h$

Δh^k = ply thickness

h = laminate thickness

The overall engineering properties of the laminate are obtained from the inversion of the stiffness matrix which yield the laminate compliances:

$$\bar{S}_{11} = \frac{1}{\bar{E}_{11}} = \frac{\bar{A}_{22}}{\bar{A}_{11}\bar{A}_{22} - \bar{A}_{12}^2}$$

$$\bar{S}_{22} = \frac{1}{\bar{E}_{22}} = \frac{\bar{A}_{11}}{\bar{A}_{11}\bar{A}_{12} - \bar{A}_{12}^2}$$

$$\bar{S}_{12} = \frac{\bar{\nu}_{12}}{\bar{E}_{11}} = \frac{\bar{\nu}_{21}}{\bar{E}_{22}} = \frac{\bar{A}_{12}}{\bar{A}_{11}\bar{A}_{22} - \bar{A}_{12}^2}$$

$$\bar{S}_{66} = \frac{1}{\bar{A}_{66}}$$

The overall engineering laminate properties for the laminate can be computed as the plies fail. As will be shown in the next section, the order of ply failure is 90° and 0°.

Initial Laminate:

$$\bar{A}_{11} = \frac{1}{2}\bar{Q}_{11}^{0^\circ} + \frac{1}{2}\bar{Q}_{11}^{90^\circ} = 11.46 \times 10^6$$

$$\bar{A}_{22} = \frac{1}{2}\bar{Q}_{22}^{0^\circ} + \frac{1}{2}\bar{Q}_{22}^{90^\circ} = 11.46 \times 10^6$$

$$\bar{A}_{12} = \frac{1}{2}\bar{Q}_{12}^{0^\circ} + \frac{1}{2}\bar{Q}_{12}^{90^\circ} = 0.48 \times 10^6$$

$$\bar{A}_{66} = \frac{1}{2}\bar{Q}_{66}^{0^\circ} + \frac{1}{2}\bar{Q}_{66}^{90^\circ} = 0.65 \times 10^{6}$$

$$\bar{S}_{11} = \bar{S}_{22} = 0.0875 \times 10^{-6} \text{ in}^2/\text{lb}$$

$$\bar{S}_{12} = -0.00366 \times 10^{-6} \text{ in}^2/\text{lb}$$

$$\bar{S}_{66} = 1.54 \times 10^{-6} \text{ in}^2/\text{lb}$$

After the 90° ply fails:

$$\bar{A}_{11} = \frac{1}{2}\bar{Q}_{11}^{0^\circ} = 10.6 \times 10^{6}$$

$$\bar{A}_{22} = \frac{1}{2}\bar{Q}_{22}^{0^\circ} = .86 \times 10^{6}$$

$$\bar{A}_{12} = \frac{1}{2}\bar{Q}_{12}^{0^\circ} = .24 \times 10^{6}$$

$$\bar{A}_{66} = \frac{1}{2}\bar{Q}_{66}^{0^\circ} = .32 \times 10^{6}$$

which can be converted to the compliances.

Maximum Strain Failure Criterion

The orthotropic ply is characterized by six ultimate strain allowables. If any one of the ultimate strains is exceeded by a ply of the laminate, the ply has failed.

Ultimate Strains:

$$\varepsilon_1 = 0.0085$$

$$-\varepsilon_1 = -0.0098$$

$$\varepsilon_2 = 0.0045$$

$$-\varepsilon_2 = -0.0090$$

$$\varepsilon_6 = 0.0150$$

$$-\varepsilon_6 = -0.0150$$

With the laminate under uniaxial loading the axial strain, ε_x, which causes failure in one of the plies can be computed by a transformation of the ultimate strains for a ply.

$$\varepsilon_x = \varepsilon_1 / (\cos^2 \theta - \bar{\nu}_{12} \sin^2 \theta)$$

$$\varepsilon_x = \varepsilon_2 / (\sin^2 \theta - \bar{\nu}_{12} \cos^2 \theta)$$

$$\varepsilon_x = \varepsilon_6 / (-2 \sin \theta \cos \theta (1 + \bar{\nu}_{12}))$$

The smallest axial strain which causes failure of any one of the plies of the laminate determines the order of ply failures. As each ply fails the laminate stiffness is recalculated to reflect the deletion of the failed ply. The ply failure strains and intermediate laminate moduli lead to a prediction of the stress strain curve and the ultimate strength.

Ply Failure Strains for 0/90 Laminate

The 90^o ply fails first by the positive transverse ultimate strain.

$$\theta = 90^o$$

$$\varepsilon_x = \varepsilon_2/(\sin^2\theta - \bar{\nu}_{12}\cos^2\theta) = \varepsilon_2 = 0.0045$$

The 0^o ply fails last by the positive longitudinal ultimate strain.

$$\theta = 0^o$$

$$\varepsilon_x = \varepsilon_1/(\cos^2\theta - \bar{\nu}_{12}\sin^2\theta) = \varepsilon_1 = 0.0085$$

Laminate Stress Strain Response

Ply Failure	ε_x	$\bar{E}_{11}$	$\Delta\varepsilon_x$	$\Delta\sigma_x = \bar{E}\Delta\varepsilon_x$	$\Sigma\Delta\sigma_x$
90^o	0.0045	11.46×10^6	.0045	51,525	51,525
0^o	0.0085	10.6×10^6	.0040	42,000	93,525

$$\therefore \sigma_o = 93,525 \text{ psi}$$

The area under the plot of ε_x versus $\Sigma\Delta\sigma_x$ yield the work to break

$$W_s = 455.0 \text{ in-lb/in}^3$$

Following the arguments of Halpin, Jerina and Johnson [1], the effective strain energy release rate will be

$$G_{1c} = A\, c_o W_b = 169 \text{ in-lb/in}^2$$

for $c_o \simeq 0.04$ in. Using Equation (1) wherein the $\bar{S}_{ij}$ terms are the initial compliances for the laminate, the apparent fracture toughness is

$$K_{lq} = \left[\frac{G_{lc}}{f(\bar{S}_{ij})}\right]^{1/2} = \left[\frac{169 \times 10^8}{12.98}\right]^{1/2} = 36.1 \text{ ksi}\sqrt{\text{in}}$$

REFERENCES

1. J. C. Halpin, K. L. Jerina, and T. A. Johnson, "Characterization of Composites for the Purpose of Reliability Evaluation", Analysis of Test Methods for High Modulus Fibers and Composites, ASTM-STP 521, August 1973, pp. 5-64.

2. W. Purcell, Private Communication, Engineering Office, Aeronautical Systems Division, Wright-Patterson Air Force Base, Ohio, 1973.

3. G. C. Sih, P. C. Paris, and G. R. Irwin, "On Cracks in Rectilinearly Anisotropic Bodies", International Journal of Fracture Mechanics, Vol. 1, 1965, pp. 189-203.

4. R. S. Rivlin and A. G. Thomas, Journal of Polymer Science, Vol. 10, 1953, pp. 291-318.

5. G. R. Irwin, Springer Encyclopedia of Physics, Vol. 6, 1958, p. 551.

6. M. E. Waddoups, J. R. Eisemann, and B. E. Kaminski, "Macroscopic Fracture Mechanics of Advanced Composite Materials", Journal of Composite Materials, Vol. 5, 1971, pp. 446-454.

7. P. H. Petit, and M. E. Waddoups, "A Method for Predicting the Nonlinear Behavior of Laminated Composites", Journal of Composite Materials, Vol. 3, 1969, pp. 1-19.

8. R. C. Novak and M. A. Decrescente, "Impact Behavior of Unidirectional Resin Matrix Composites Tested in the Fiber Direction", Composite Materials: Testing and Design (Second Conference), ASTM-STP 497, April 1973, pp. 311-323.

9. C. C. Chamis, M. P. Hanson, and T. T. Serafini, "Impact Resistance of Unidirectional Fiber Composites", Composite Materials: Testing and Design (Second Conference), ASTM-STP 497, April 1973, pp. 324-349.

TABLE 1 - MATERIAL DATA

	FIBER	ULTIMATE TENSILE STRENGTH (KSI)	TENSILE MODULUS (MSI)	ULTIMATE STRAIN (%)
TYPE I	HMS	300	55	0.545
TYPE II	HTS	400	38	1.05
	MODMOR II	380	40	.95
TYPE III	A-S	400	30	1.33
	E-GLASS	400	10.5	3.0
	RESIN			
	ERL 2256	15.2	0.6	6.5
	ERLA 4617	14.8	0.78	2.2
	HERCULES 3004	10.2	0.36	50.0
	3 M 1002	6.14	0.474	---
	PPQ 401	13.1	0.46	---

TABLE 2 - IMPACT DATA

Specimen No.	Material	Width (in)	Thickness (in)	Projectile Diameter (in)	Projectile Mass (gm)	Vel. (ft/sec)	K.E.* (ft/lbs)	K.E./t	σ_R (KSI)	σ_R/σ_o
2-6889	Scotchply	1.0	0.102	0.177	0.350	483	2.66	26.1	63.4	~1.0
2-6890	↓	↓	0.102	↓	↓	524	3.17	31.1	58.9	0.985
1-6883	↓	↓	0.091	↓	↓	681	5.51	60.5	55.9	0.859
2-6891	↓	↓	0.102	↓	↓	775	7.16	70.1	47.7	0.797
3-7134	↓	↓	0.107	↓	↓	1006	12.10	113.0	39.4	0.695
3-7133	↓	↓	0.105	↓	↓	1013	12.30	117.0	41.6	0.732
3-7135	↓	↓	0.107	↓	↓	1067	13.70	128.0	37.5	0.660
4-7097	↓	1.5	0.104	↓	↓	754	6.78	65.2	59.8	0.920
4-7096	↓	↓	0.102	↓	↓	758	6.85	67.2	55.4	0.852
4-7098	↓	↓	0.103	↓	↓	880	9.30	90.3	53.6	0.824
4-7099	↓	↓	0.104	↓	↓	904	9.80	94.3	55.2	0.850
0-6358	↓	0.5	0.097	↓	↓	150	0.194	2.00	74.9	0.978
0-6360	↓	↓	↓	↓	↓	175	0.275	2.84	73.6	0.961
0-6359	↓	↓	↓	↓	↓	176	0.287	2.95	74.5	0.973
0-6362	↓	↓	↓	↓	↓	257	0.634	6.54	80.2	~1.0
0-6361	↓	↓	↓	↓	↓	290	0.836	8.63	75.8	0.990
0-6363	↓	↓	↓	↓	↓	294	0.863	8.90	80.7	~1.0
0-6365	↓	↓	↓	↓	↓	377	1.505	15.55	64.2	0.840
0-6364	↓	↓	↓	↓	↓	402	1.727	17.80	69.5	0.910
0-6366	↓	↓	↓	↓	↓	410	1.818	18.75	74.5	0.975
0-6369	↓	↓	↓	↓	↓	498	2.772	28.60	59.8	0.782
0-6367	↓	↓	↓	↓	↓	500	2.79	28.80	56.7	0.742
0-6368	↓	↓	↓	↓	↓	500	2.79	28.80	59.2	0.774

*Adjusted for Rebound Velocity

TABLE 2 - (Continued)

Specimen No.	Material	Width (in)	Thickness (in)	Projectile Diameter (in)	Projectile Mass (gm)	Vel. (ft/sec)	K.E.* (ft/lbs)	K.E./t	σ_R (KSI)	$\sigma_R/\dot{\sigma}_o$
2-6887	Scotchply	1.0	0.104	0.250	1.024	271	2.50	24.0	49.4	0.825
2-6888	↓	↓	0.105	↓	↓	272	2.51	23.9	67.4	~1.0
2-6886	↓	↓	0.106	↓	↓	301	3.13	29.5	41.3	0.691
1-6885	↓	↓	0.094	↓	↓	303	3.16	33.6	75.3	~1.0
1-6880	↓	↓	0.093	↓	↓	450	7.11	76.5	36.2	0.557
1-6882	↓	↓	0.092	↓	↓	458	7.36	80.0	39.6	0.609
1-6881	↓	↓	0.090	↓	↓	460	7.45	82.8	36.9	0.568
3-7136	↓	1.5	0.109	↓	↓	447	7.02	64.4	56.12	0.986
3-7137	↓	↓	0.110	↓	↓	457	7.33	66.6	45.97	0.809
A1-6191	A-S/4617	0.5	0.140	0.177	0.350	301	0.915	6.53	85.4	0.980
A1-6192	↓	↓	0.140	↓	↓	293	0.860	6.14	85.9	0.986
A1-6193	↓	↓	0.139	↓	↓	385	1.68	12.10	74.4	0.855
A1-6194	↓	↓	0.139	↓	↓	400	1.82	13.10	70.6	0.811
A1-6195	↓	↓	0.139	↓	↓	387	1.70	12.25	73.0	0.838
A1-6196	↓	↓	0.142	↓	↓	501	2.95	20.75	64.0	0.735
A1-6197	↓	↓	0.139	↓	↓	518	3.15	22.60	48.5	0.558
A1-6198	↓	↓	0.138	↓	↓	528	3.28	23.70	56.3	0.646
A2-4433	↓	1.0	0.145	↓	↓	304	0.94	6.48	105.9	~1.0
A2-4434	↓	↓	0.144	↓	↓	449	2.35	16.3	99.4	0.937
A2-4435	↓	↓	0.144	↓	↓	451	2.37	16.45	101.9	0.960
A2-4436	↓	↓	0.141	↓	↓	601	4.31	30.6	81.2	0.766
A2-4437	↓	↓	0.140	↓	↓	598	4.30	30.7	87.9	0.828

TABLE 2 - (Continued)

Specimen No.	Material	Width (in)	Thickness (in)	Projectile Diameter (in)	Projectile Mass (gm)	Vel. (ft/sec)	K.E.* (ft/lbs)	K.E./t	σ_R (KSI)	$\sigma_R/\dot{\sigma}_o$
A3-4473	A-S/4617	1.0	0.069	0.177	0.350	303	0.945	13.7	136.0	~1.0 (edge-bad)
A3-4474			0.075			303	0.945	12.6	107.1	0.935
A3-4475			0.070			437	2.21	31.6	129.5	~1.0 (edge-bad)
A3-4476			0.072			462	2.48	34.4	104.5	0.912
A3-4477			0.070			597	4.29	61.2	68.3	0.598
A3-4478			0.074			567	3.86	52.2	69.3	0.605
A4-6370	A-S/3004	0.5	0.059			162	0.065	1.10	76.3	0.813
A4-6371			0.062			166	0.081	1.31	73.3	0.782
A4-6372			0.065			169	0.093	1.43	86.0	0.918
A4-6374			0.070			280	0.772	11.05	62.3	0.665
A4-6375			0.070			312	1.00	14.3	55.7	0.595
A4-6377			0.073			409	1.91	26.1	36.9	0.394
A4-6378			0.072			386	1.67	23.2	36.8	0.393
A4-6379			0.073			493	2.85	39.1	19.9	0.212
A4-6380			0.072			498	2.90	40.2	0	0
A4-6381			0.075			466	2.54	33.9	16.6	0.177
HM-6233	HMS/4617		0.115			163	0.069	0.60	49.7	0.763
HM-6234						152	0.027	0.235	44.6	0.685
HM-6235						164	0.074	0.643	36.7	0.564
HM-6231						317	1.045	9.10	26.7	0.410
HM-6232						309	0.985	8.57	30.6	0.470
HM-6229						400	1.820	15.70	0	0
HM-6228						401	1.825	15.75	0	0
HM-6226						528	3.30	28.70	17.0	0.261 } Penetration
HM-6227						524	3.25	28.25	15.5	0.238 }

TABLE 2 - (Continued)

Specimen No.	Material	Width (in)	Thickness (in)	Projectile Diameter (in)	Projectile Mass (gm)	Vel. (ft/sec)	K.E.* (ft/lbs)	K.E./t	σ_R (KSI)	$\sigma_R/\dot{\sigma}_o$
HT-6355	HTS/4617	0.5	0.115	0.177	0.350	165	0.077	0.670	72.1	0.820
HT-6356						151	0.024	0.285	89.5	~1.0
HT-6357						170	0.097	0.844	84.6	0.963
HT-6352						316	1.04	9.05	65.2	0.740
HT-6353						302	0.935	8.14	70.5	0.802
HT-6354						312	1.01	8.79	50.8	0.578
HT-6349						378	1.60	13.93	45.6	0.520
HT-6350						371	1.54	13.40	57.5	0.655
HT-6351						410	1.92	16.70	60.6	0.690
HT-6346						515	3.14	27.30	27.5	0.313
HT-6347						518	3.17	27.60	30.9	0.350
HT-6348						511	3.09	26.90	16.4	0.186
MII-6144	MODII/4617		0.131			176	0.122	0.930	52.4	0.770
MII-6145			0.130			161	0.062	0.477	50.2	0.740
MII-6146			0.129			161	0.062	0.481	60.5	0.890
MII-6147			0.131			298	0.91	6.940	46.9	0.689
MII-6148			0.133			290	0.85	6.390	53.1	0.780
MII-6149			0.131			293	0.87	6.650	59.9	0.882
MII-6150			0.130			473	2.61	20.10	21.5	0.316
MII-6151			0.131			465	2.51	19.15	30.9	0.455
MII-6152			0.130			461	2.48	19.10	31.9	0.469
MII-6153			0.131			541	3.48	26.55	21.7	0.319
MII-6154			0.130			596	4.22	32.50	3.9	0.057
MII-6155			0.131			610	4.42	33.70	15.0	0.220

TABLE 2 - (Concluded)

Specimen No.	Material	Width (in)	Thickness (in)	Projectile Diameter (in)	Projectile Mass (gm)	Vel. (ft/sec)	K.E.* (ft/lbs)	K.E./t	σ_R (KSI)	$\sigma_R/\dot{\sigma}_o$
MII-6165	MODII/2256	0.5	0.105	0.177	0.350	163	0.069	0.657	93.2	~1.0
MII-6166						162	0.065	0.619	77.6	~1.0
MII-6167						155	0.038	0.362	83.7	~1.0
MII-6162						299	0.903	8.60	53.7	0.688
MII-6163						301	0.915	8.72	54.9	0.704
MII-6164						297	0.890	8.47	46.5	0.597
MII-6160						412	1.94	18.50	20.2	0.259
MII-6161						427	2.09	19.90	23.8	0.305
MII-6159						447	2.30	21.90	8.5	0.109
MII-6156						608	4.39	41.80	12.4	0.159 } Penetration
MII-6157						596	4.22	40.10	8.5	0.109 }
MII-6158						585	4.06	38.70	10.0	0.128 }
MII-6382	MODII/PPQ		0.077			170	0.097	1.26	91.1	~1.0
MII-6383						125	0.00	0	72.9	~1.0
MII-6384						301	0.915	11.90	36.4	0.524
MII-6385						306	0.955	12.40	54.5	0.785
MII-6386						345	1.30	16.85	38.5	0.555
MII-6387						401	1.82	23.60	17.4	0.251
MII-6388						498	2.98	38.75	0	0
MII-6389						503	3.04	39.50	0	0

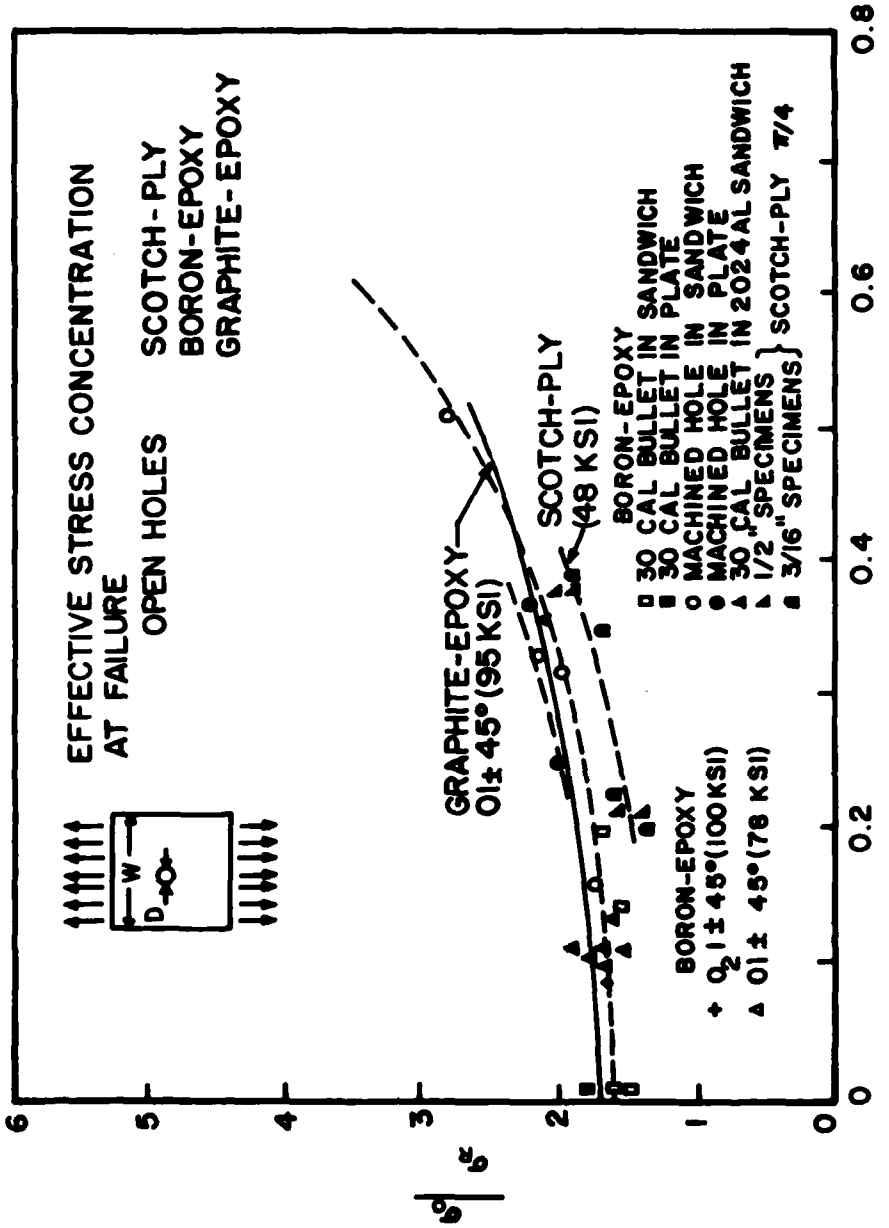

Figure 1. Comparison Between Strength Reduction Produced By A Drilled Hole and the Strength Reduction Produced By A Bullet

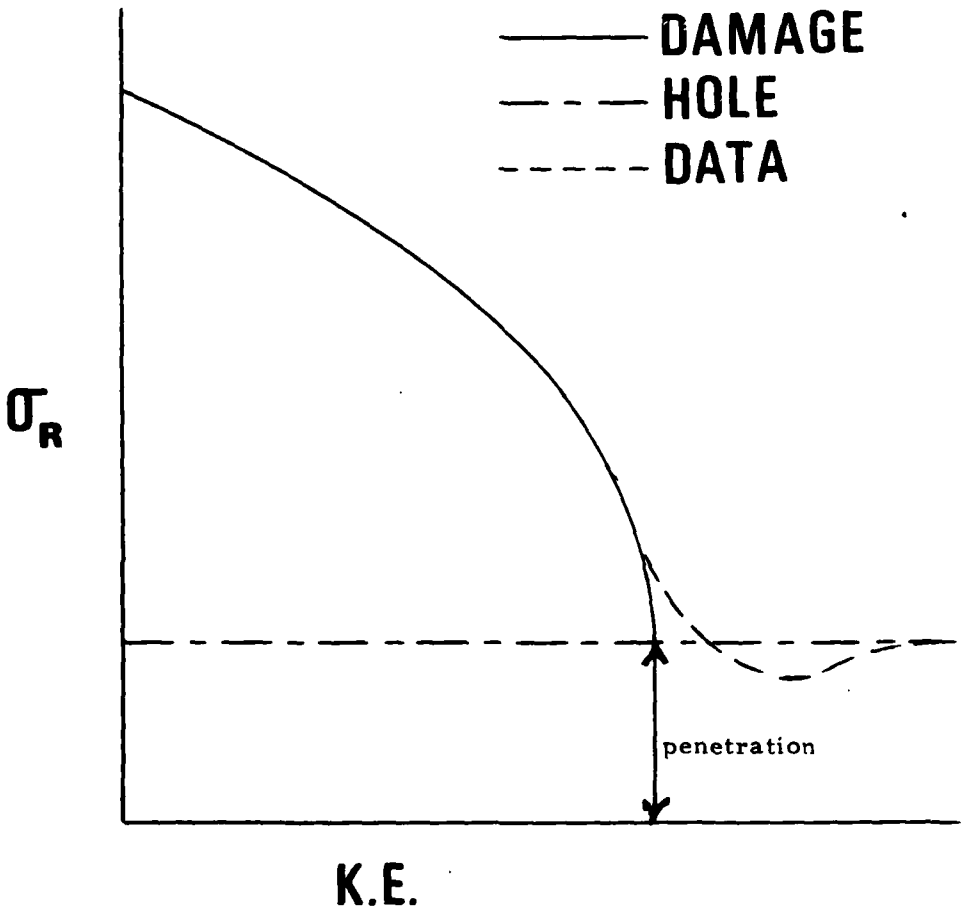

Figure 2. Residual Strength As A Function of Kinetic Energy

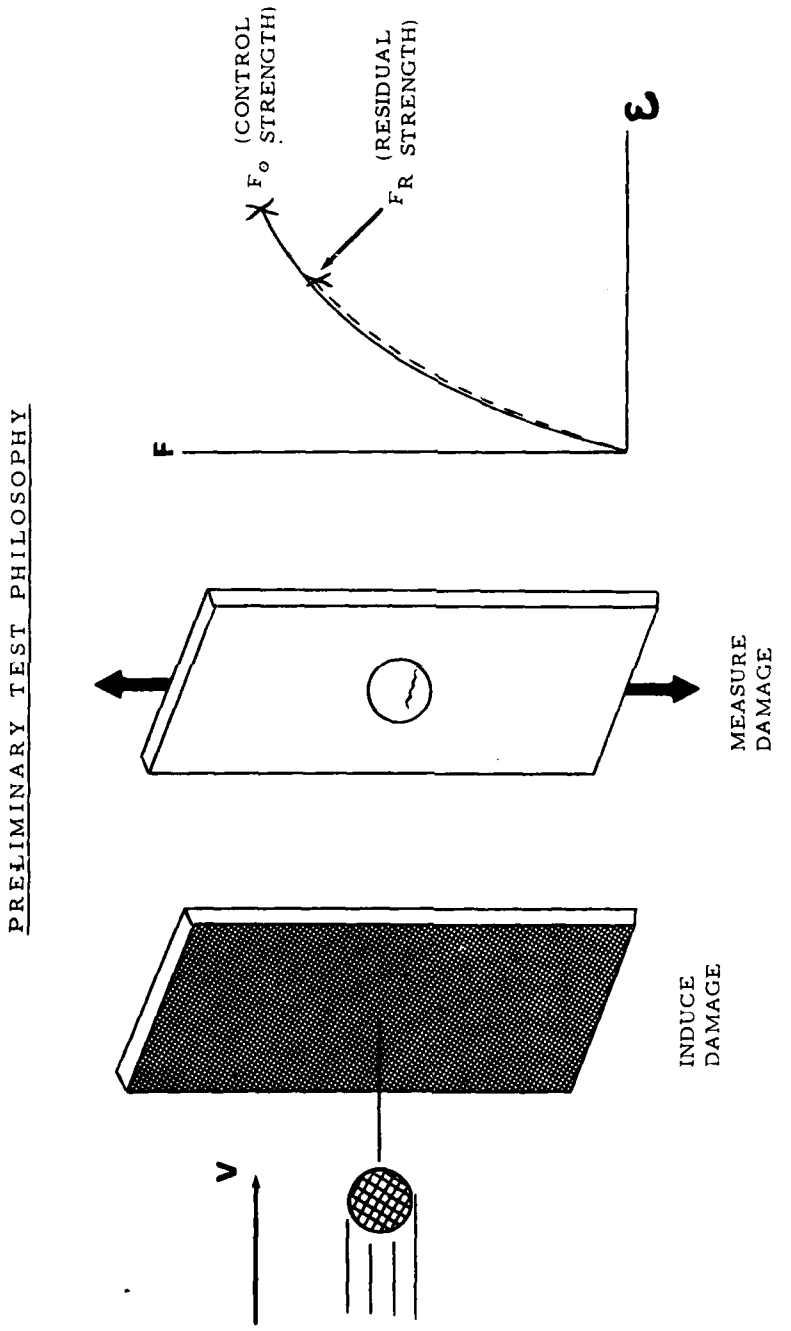

Figure 3. Schematic of Residual Strength Analogy

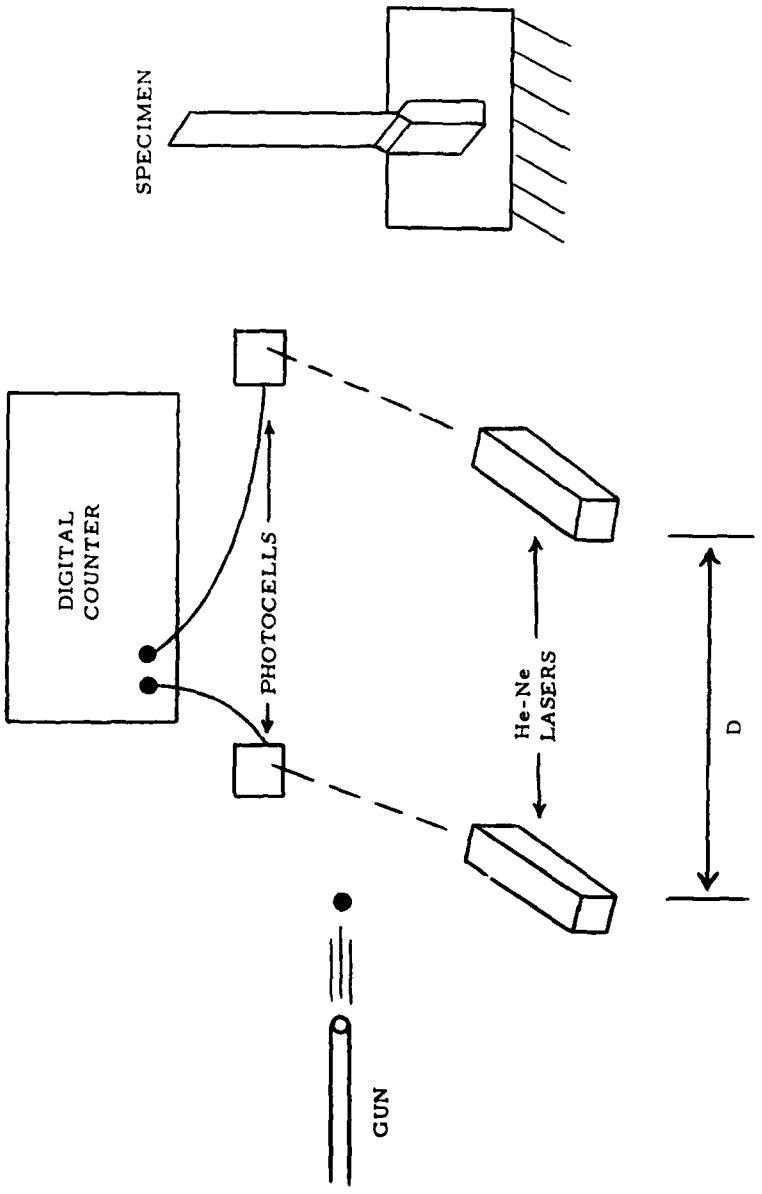

Figure 4. Schematic of Experimental Set-up

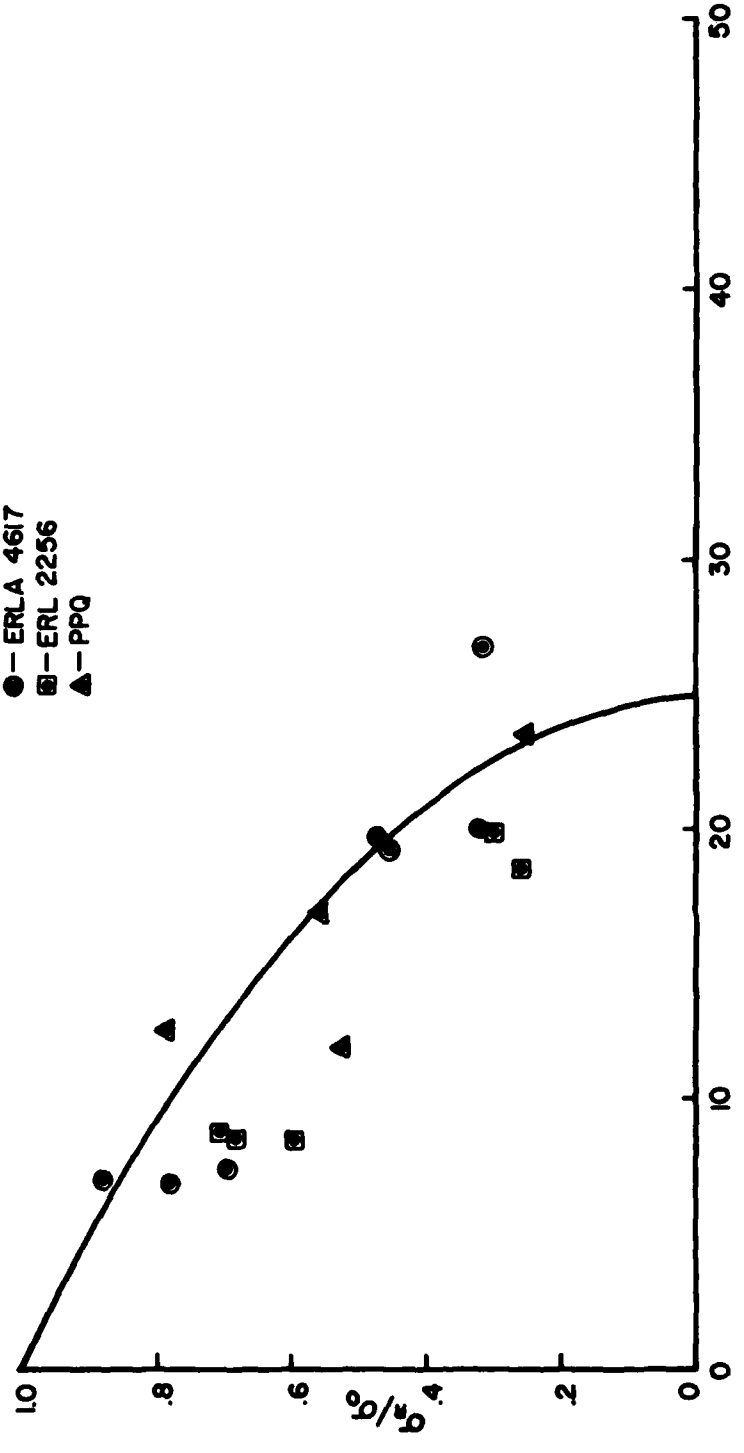

Figure 5. Effect of Matrix on Impact Residual Strength (MOD II Fiber)

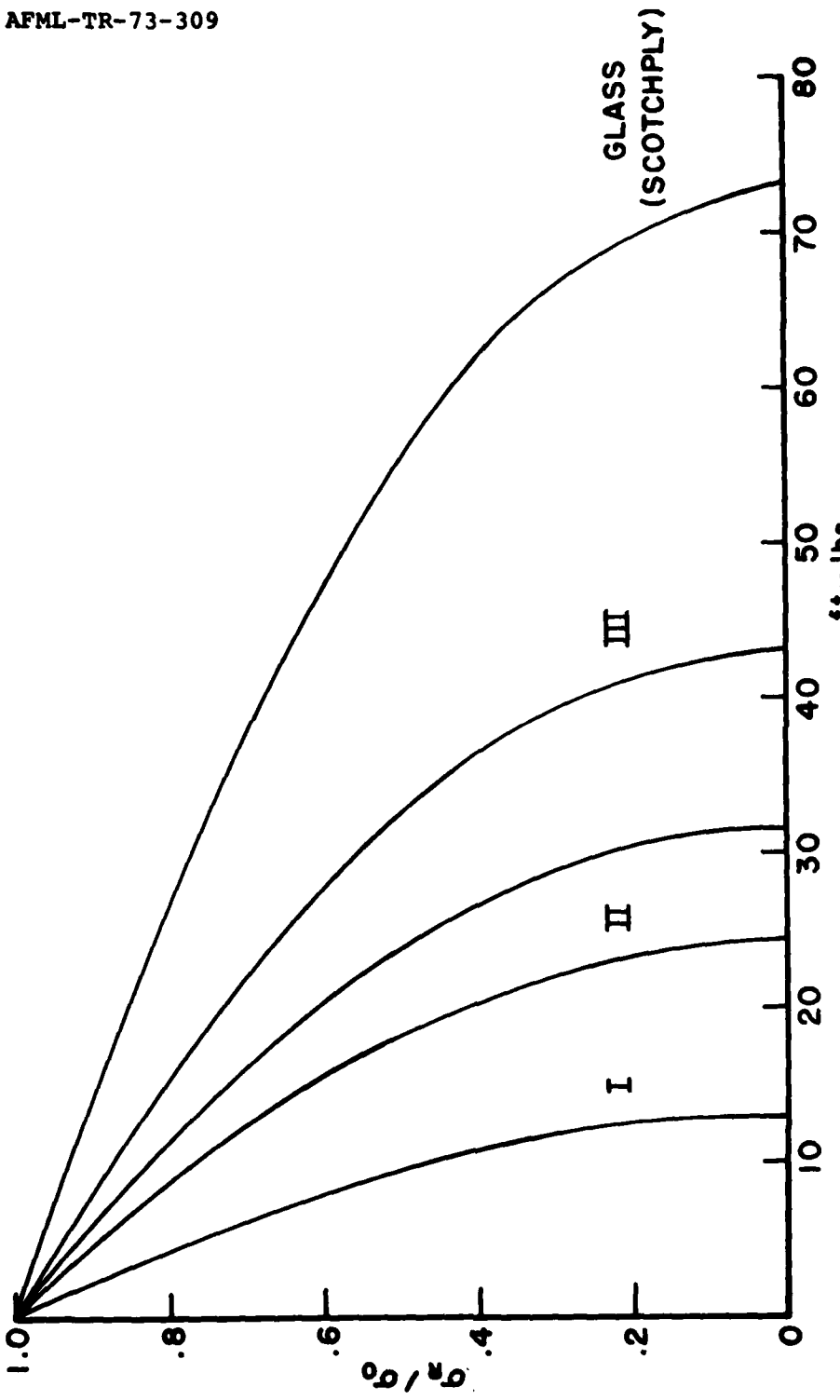

Figure 6. Effect of Fiber on Impact Residual Strength (Fiber Data in Table 1, ERL 4617 Resin System Used in All Cases)

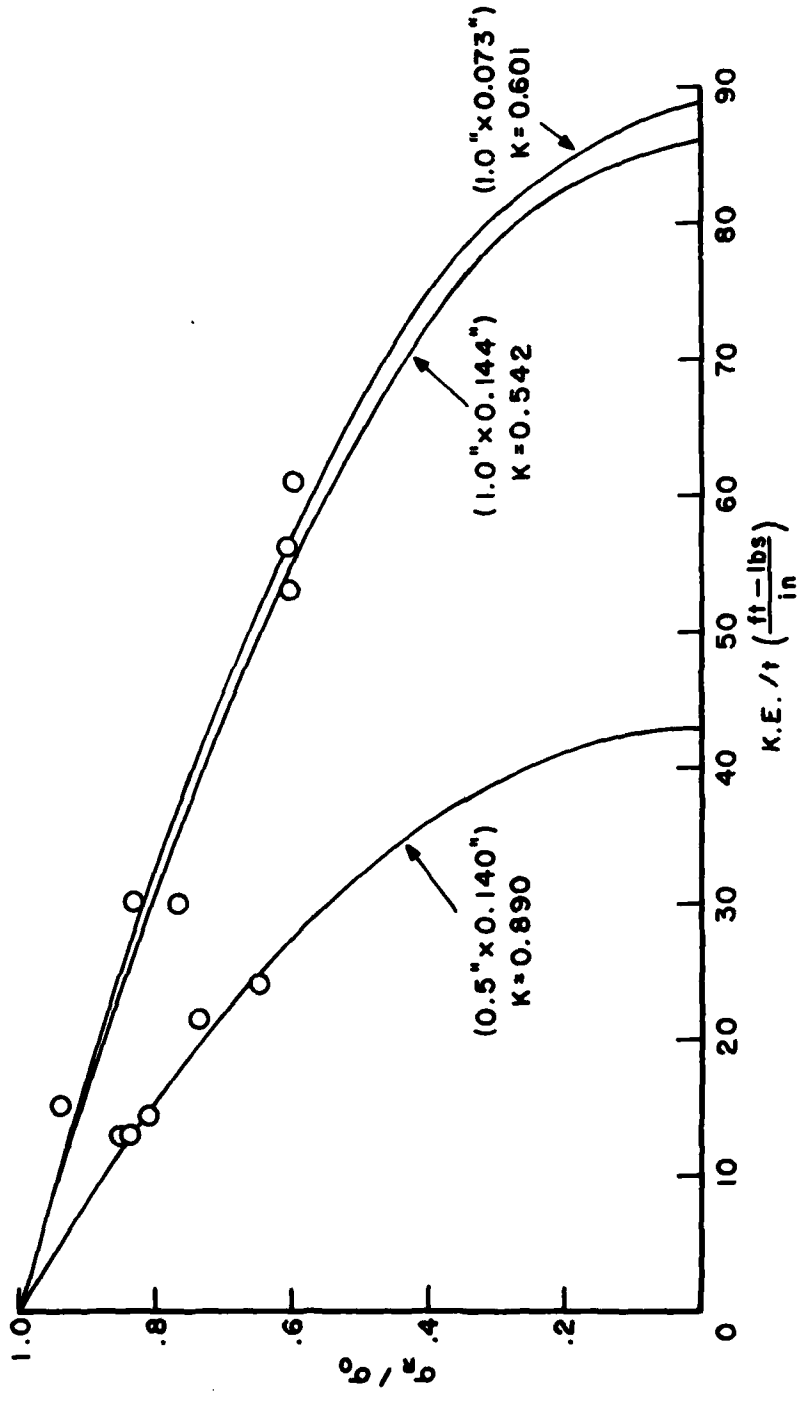

Figure 7. Effect of Specimen Size on Impact Residual Strength (A-S/4617 Composites)

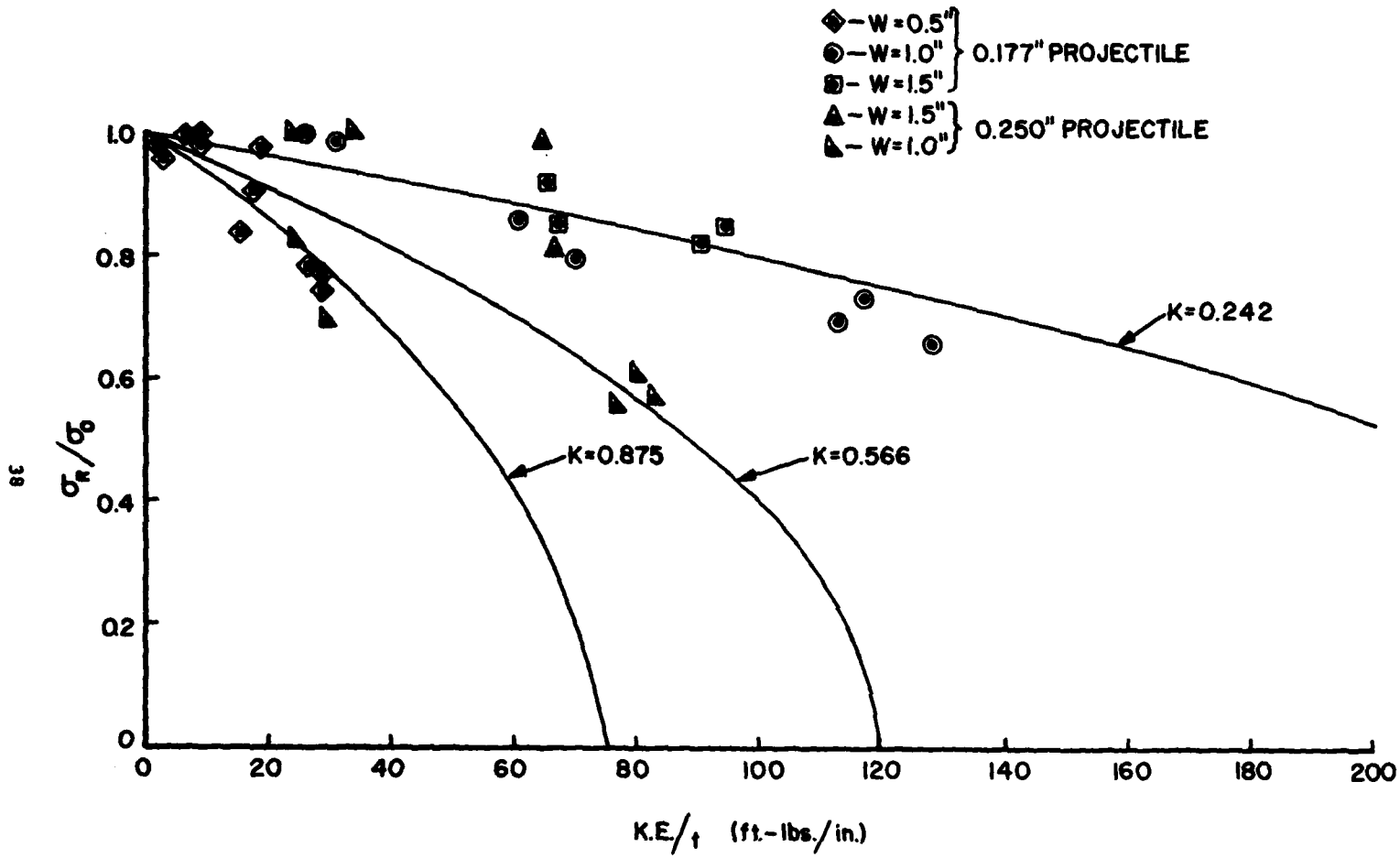

Figure 8. Effect of Specimen Width to Projectile Diameter on Impact Residual Strength (Scotchply/1002 Composites)

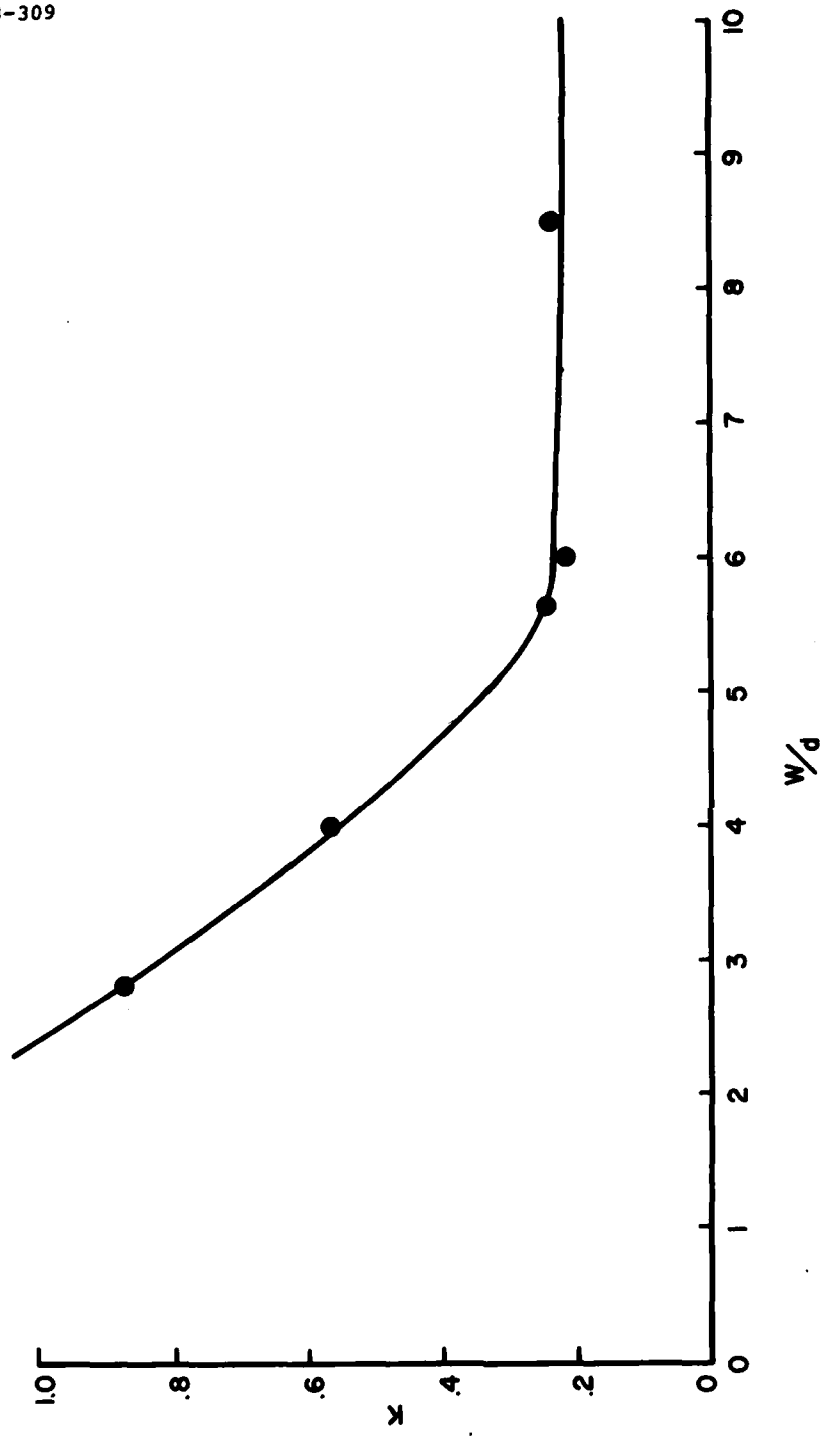

Figure 9. Effect of Specimen Width to Projectile Diameter on the Value of K (Scotchply/1002 Composites)

UNCLASSIFIED

Security Classification

DOCUMENT CONTROL DATA - R & D

(Security classification of title, body of abstract and indexing annotation must be entered when the overall report is classified)

1. ORIGINATING ACTIVITY (Corporate author)	2a. REPORT SECURITY CLASSIFICATION
Air Force Materials Laboratory Wright-Patterson AFB, Ohio 45433	UNCLASSIFIED 2b. GROUP

3. REPORT TITLE

Residual Strength Characterization of Laminated Composites Subjected to Impact Loading

4. DESCRIPTIVE NOTES *(Type of report and inclusive dates)*

5. AUTHOR(S) *(First name, middle initial, last name)*

George E. Husman
James M. Whitney
John C. Halpin

6. REPORT DATE	7a. TOTAL NO. OF PAGES	7b. NO. OF REFS
February 1974	44	9

8a. CONTRACT OR GRANT NO.	9a. ORIGINATOR'S REPORT NUMBER(S)
b. PROJECT NO.	AFML-TR-73-309
c.	9b. OTHER REPORT NO(S) *(Any other numbers that may be assigned this report)*
d.	

10. DISTRIBUTION STATEMENT

Approved for public release; distribution unlimited.

11. SUPPLEMENTARY NOTES	12. SPONSORING MILITARY ACTIVITY
	Air Force Materials Laboratory (LBC) Wright-Patterson AFB, Ohio 45433

13. ABSTRACT

An analogy between damage inflicted by a single point hard particle impact and damage inflicted by inserting a flaw of known dimensions in a static tensile coupon is discussed. The results suggest that residual strength can be predicted as a function of kinetic energy of impact by executing two experiments, a static tensile test on an unflawed specimen and a static tensile test on a coupon previously subjected to a single point impact. The model appears to be accurate for impact velocities which are less than the penetration velocity. For velocities above complete penetration, the residual strength is identical to the static strength of a coupon with a hole having the same diameter as the impacting particle. Comparison of various materials indicates that the impact strength of composite materials is strongly influenced by the strain energy to failure of the reinforcement.

DD FORM 1 NOV 68 1473

UNCLASSIFIED

Security Classification

UNCLASSIFIED

Security Classification

14. KEY WORDS	LINK A		LINK B		LINK C	
	ROLE	WT	ROLE	WT	ROLE	WT
Composites						
Impact						
Fracture Analysis						

UNCLASSIFIED

Security Classification

*U.S.Government Printing Office: 1974 — 758-433/513